Environmental Challenges 4 (2021) 100168

Contents lists available at ScienceDirect

Environmental Challenges

journal homepage: www.elsevier.com/locate/envc

Urban sprawl and its impact on land use land cover dynamics of Sekondi-Takoradi metropolitan assembly, Ghana

Ernest Biney*, Ebenezer Boakye

Department of Civil Engineering, Takoradi Technical University, P.O. Box 256, Takoradi, Ghana

ARTICLE INFO

Keywords:
Land use
Remote sensing
Shannon's entropy
Urban sprawl

ABSTRACT

In Ghana, Sekondi-Takoradi has been one of the preferred cities for many people due to the prevalence of industries, the presence of harbor, and the airport. However, the discovery of oil off the coast of the Western region, where Sekondi-Takoradi is the administrative and economic capital makes it more attractive to people in the area. This has increased the number of urban dwellers and resulted in the conversion of different and Land Use /Land Cover (LULC) forms into urban or built-up areas. Using Landsat imageries from 1991, 2002, 2008, and 2018 of Sekondi-Takoradi, together with geospatial and Shannon's entropy techniques, this paper assesses the impact of urban sprawl on land use and land use dynamics within the metropolis. Results of land use land cover change showed significant changes during the period of study. Settlement increased by 25.93% whereas water, vegetation, and bare land reduced by 0.08%, 16.00%, and 9.86% respectively. This reveals the occurrence of an unguided expansion of built-up area in the metropolis. Also, results from entropy calculations showed high entropy values ranging from 2.42 to 2.50, though the entropy values did not significantly change throughout the study. This indicates that the metropolis has been experiencing sprawl from 1991 to 2018 and thus urban development has significantly changed the land cover stratum of the metropolis. The findings demonstrate the value of spatial modeling in environmental management and urban planning.

1. Introduction

Since time immemorial, the earth's surface has been changing at different spaces and time scales. These changes, of which some take place at a short time and others at longer years are caused by natural phenomena and human activities (Zhou and Chen, 2018). Human activities such as using fire for hunting and clearing of land for farming, and building and construction bring changes to the earth's land surface; while natural phenomena like drought, flooding, earthquake, and volcanic eruption also bring changes to the earth land surface (Garg et al., 2019). Even though the natural process may bring about changes in land cover, the majority of the changes in land cover are human-induced (Garg et al., 2019; Mohamed et al., 2020). The present rates and extent of land cover changes are higher than ever recorded in history; this is causing numerous changes in the ecosystem (Appiah et al., 2017).

In recent times, industries and developments are increasing the population of urban dwellers and urban centers. The increase in urban population and urban centers are changing vegetative lands or land covers into impervious surfaces. Although these conversions and their effects are globally found in metropolitan areas, it is becoming a disaster in developing countries (Appiah et al., 2017; Li et al., 2018). Expansion of urban centers has increased the transformation of natural resources and altered the pattern of land cover and land use. Wandl and Magoni (2017), reported that about 50% of the world's population now lives in urban centers and this is making the urban landscapes relatively the fastest land cover type. According to Dominguez et al. (2018), the world population is anticipated to go up from the previous estimate of 6.8 billion in 2009 to 9.1 billion by the year 2050 and the urban population is anticipated to rise from 3.4 billion in 2009 to 6.3 billion by 2050. As the number of people living in the urban centers goes up, the peripheries are targeted as an escape from congestion and problems that emanate from overpopulation (Guzmán et al., 2017). This deforms the land cover pattern at the peripheries through the pressure and the transformation it undergoes (Li et al., 2018). In developing countries, urban expansion negatively affects agricultural lands which are essential factors in determining land use and land cover change (Li et al., 2018; Yu et al., 2018). Issues of urban sprawl have not only given rise to new methods in attaining a suitable urban form, but also to new techniques used to monitor and analyze urban sprawl and its effects (Mosammam et al., 2017). To monitor and analyze urban sprawl, some researchers propose using sprawl indicators whereas other researchers emphasize the use of geospatial techniques such as remoting sensing and GIS in addition to statistical techniques (Yang et al., 2018). The use of GIS and remote sensing techniques has proven to be effi-

* Corresponding author at: Department of Civil Engineering, Takoradi Technical University, P.O. Box 256, Takoradi, Ghana.
E-mail address: ernest_biney@yahoo.com (E. Biney).

https://doi.org/10.1016/j.envc.2021.100168
Received 9 April 2021; Received in revised form 1 June 2021; Accepted 1 June 2021

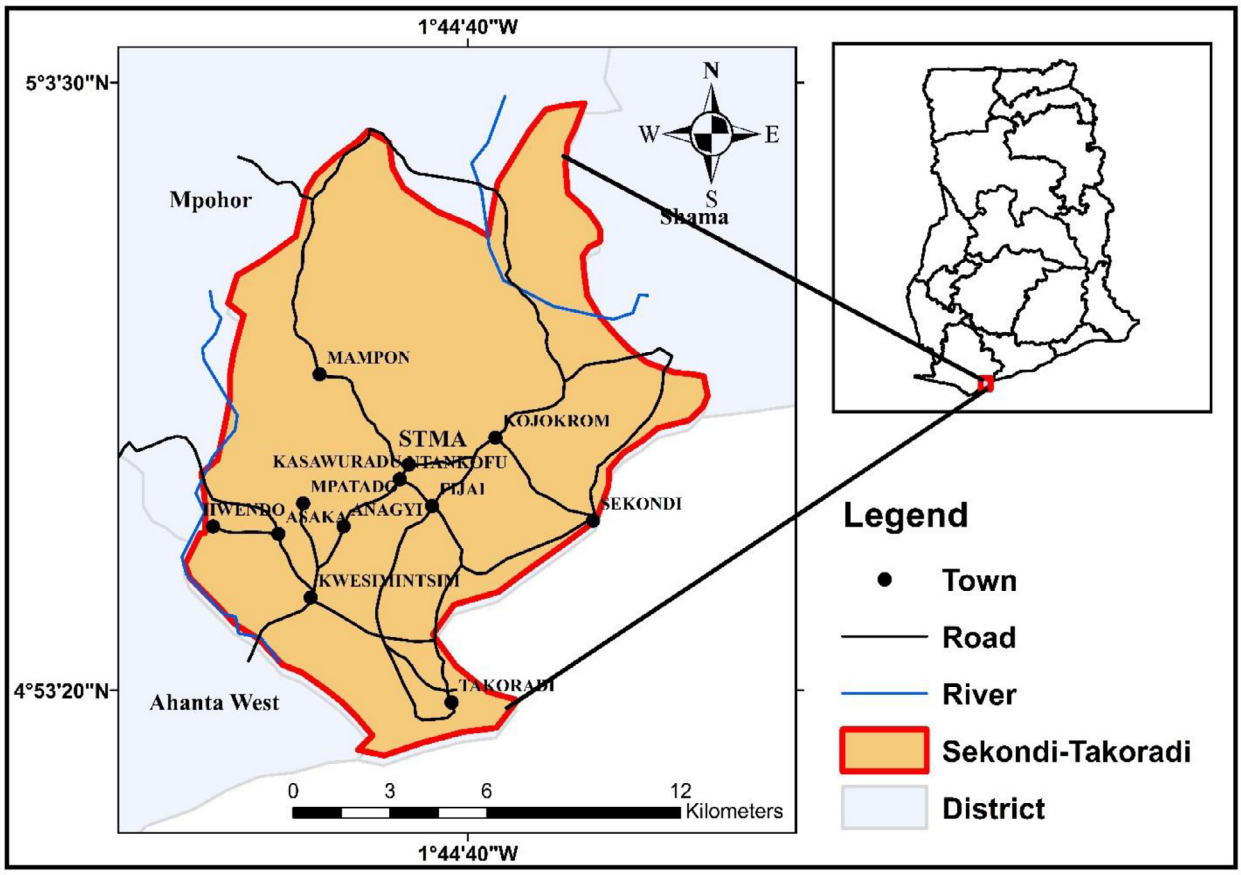

Fig. 1. Map of the study area.

cient in monitoring, mapping, and assessing urban sprawl and in LULC changes.

Sekondi-Takoradi has over the years seen changes in its land use and land cover due to the increasing urban expansion and impervious surface taking place in the metropolis. The presence of the harbor increased the number of urban dwellers and attracted a lot of industries into the metropolis (Fiave, 2017). These urban dwellers and industries demanded land for their residential and industrial purposes and therefore put pressure on the land available, resulting to changes in the land cover characteristics. Additionally, the discovery of oil in the Western Region, where Sekondi-Takoradi is the district capital and serves as a suitable place for oil industries due to the availability of the harbor has brought serious transformations to the land cover. In 1970, the population of Sekondi-Takoradi was 135,760 but increased to 559,548 in 2010 (Fiave, 2017; Obeng-Odoom, 2014; Stemn and Agyapong, 2014; Eduful and Hooper, 2019). The increase in the city's urban population has brought pressure on the land cover causing environmental problems. It is for this reason that this study seeks to assess the impact of urban sprawl on the land use and land cover in Sekondi-Takoradi.

This paper is sectioned mainly into introduction, materials and methods, results and discussions, and conclusion. However, some main sections are further organized into subsection headings.

2. Materials and methods

2.1. Study area

Sekondi-Takoradi Metropolis (Fig. 1) comprises of cities of Sekondi and Takoradi in the Western region. It lies between Latitude 4° 52′ 30″ N and 5° 04′ 00″ N and Longitudes 1° 37′ 00″ W and 1° 52′ 30″W. The Metropolis is bordered by Ahanta West District at the west, Shama District at the east, the Atlantic Ocean at the south and Wassa East district at the north. It is also the administrative capital of the western region and has an area size of about 191.7 km^2. Though it is the smallest district in terms of land size, Sekondi-Takoradi Metropolis is the most urbanized among the districts in the region (Assembly, 2010; Chatwin, and Arku, 2018). According to the 2010 Population and Housing Census, the Metropolis has a population of 559,548 and was projected to increase to 946,000 in the year 2020 (Tarkang et al., 2019). With the total population, 96.1% live in urban localities and 3.9% live in rural localities. This proves that a large number of the people living within the metropolis live in urban areas (Service, 2014).

The Metropolis serves as an industrial and commercial center and this attracts migrants across the nation to the Metropolis. Takoradi, for instance, houses about 10.2% of all industrial establishments across the country (Obeng-Odoom, 2019). Industries such as timber, plywood, shipbuilding, railway repair and oil industries are major industries found in Sekondi-Takoradi (Adjei Mensah et al., 2019). The topography of the Metropolis is of diverse landscape. The coastline is made up of capes and bays which have been largely eroded (Aduah and Mantey, 2020). The metropolis has two main rivers; the Whin River and the Kansaworado River. The climate of the Metropolis is equatorial, with an average annual temperature of about 22 °C, experienced between January and March. Rainfall is bi-modal, with the major season occurring between March and July and the minor season occurring between August and November. The mean annual rainfall is about 1380 mm, covering an average of 122 rainy days (Aduah and Mantey, 2020).

2.2. Data

The data used for the study are shown in Table 1. They are categorized into reference data and remote sensing (RS) data. The remote

Table 1
Data used for the study.

Remote sensing data	Resolution	Date acquired	Source	No. of bands
Landsat TM	30 m	01/01/1991	USGS	7
Landsat ETM+	30 m	15/01/2002	USGS	8
Landsat ETM+	30 m	03/01/2008	USGS	8
Landsat OLI/TRIS	30 m	18/01/2018	USGS	11
Reference data				
Google earth images		1991, 2002, 2008 and 2018	Google earth explorer	
Land cover maps		1991, 2008,2018	Forestry Department, Ghana	

sensing data used were time series of Landsat images; Thematic Mapper (TM), Enhanced Thematic Mapper Plus (ETM+), and Operational Land Imager (OLI) and Thermal Infrared Sensor (TIRS) obtained in the years of 1991, 2002, 2008, 2018. The Landsat images were acquired from U.S. Geological Survey earth explorer with a criterion of images having less than 10% cloud cover. The Landsat images used had a path and row of 194/57. As indicated in Table 1, the 1991 image was a Landsat 4 Thematic Mapper image, 2002 and 2008 images were Landsat 7 Enhanced Thematic Mapper plus images and the 2018 image was a Landsat 8 Operational Land Image and Thermal Infrared Sensor (OLI/TIRS) image. The spectral and spatial resolution of the obtained images was 30 × 30 m and this was similar to all the images, therefore, the images were used to define the purposes of the study. Four images were used for the study to have a better understanding of how the land cover has changed over the years, however, the inconsistency in the image intervals was due to the lack of data with a cloud cover of less than 10%. High-resolution Google earth images of 1991, 2002, 2008, and 2018, and land cover maps were used in training and in assessing the accuracy of the classes during classification. Reference data were used for training and accuracy assessment during classification.

2.3. Image pre-processing and classification

The images obtained from the Landsat satellite were in Tier 1 and Tier 2. The Tier 1 images of 2002, 2008, and 2018 were geometrically corrected from source and geo-referenced to 1984 World Geodetic System Universal Transverse Mercator Zone 30 North Projection (UTM '84 zone 30 N). The Tier 2 image of 1991 was not pre-processed from the source, so there was the need to geometrically correct and register the image to UTM 84 zone 30 N to ensure a uniform projection. The georeferencing of the 1991 image was done in QGIS 2.18.12 software using ground control points (GCP) of (2019) recent images from google earth. A root means square which is half the pixel cell size was achieved from the geo-referenced image of 1991. In geo-referencing the 1991 image, Nearest-Neighbour re-sampling method was used due to its ability to maintain the pixel values of the original image. There was no radiometric correction done on the images because the images were already corrected from the source. Using the clipper tool in QGIS, the study area for all the satellite images was extracted for further processing and analysis since they were the regions of interest. Sub-setting in QGIS can be done either by using a polygon shapefile as a mask layer or by specifying directly the area of extent. In this study, subsets were done using a vector polygon shapefile. The subset images were band stacked and saved as separate files in a Geo-TIF format. True color composite and false color composite were jointly used to identify the land cover classes on the images in the Google earth engine for image classification. Image classification is done to point out and allot thematic classes in the real world to the image pixels. In this study, the classification was done by first acquiring training samples, creating training sites, and employing the supervised classification technique to classify the images into their respective classes. The supervised classification was chosen due to its ability in using training samples to identify a particular land cover type as well as giving analysts full control of the process. Being familiar with the study area through field experience, knowledge from literature, and based on the images spectral characteristics as well as using a standard classification scheme such as Anderson's classification scheme and local factors; the classes identified were: Water, Vegetation, Bare land, Built-up or Settlement. These classes are explained in Table 2.

The identified land cover classes were trained from the images in the google earth engine using a signature editor tool. The random forest algorithm or classifier under the supervised classification in the google earth engine was used to classify the images into four classes. Random forest was chosen due to its usefulness in calculating important information about errors, variable importance, and data outliers. Such information can be used to assess the performance of the model and make changes to the training data if necessary (Hong et al., 2019) Also, with Random forest, two-thirds of the training data is used to build the random forest model while one-third of training data is used to calculate the error of prediction. This makes it easier to assess the accuracy portion of each analysis.

2.4. Accuracy assessment

Assessing the quality of results after classification is performed from satellite images is very important for change detection analysis (Othow et al., 2017). Accuracy assessment shows the level of confidence between the classified images and the reference data to know how accurately the classified satellite image agrees with the reference data (Mosammam et al., 2017). In this study, an accuracy assessment was conducted on the classified images of 1991, 2002, 2008, and 2018 to determine the quality of classification information obtained. Independent sample points selected from reference data (such as GPS coordinates of the study area and aerial photographs) were used to ascertain the classification accuracy for this study. A total random point of four hundred and eighty was extracted from aerial photographs of 1991, 2002, 2008, and 2018 to perform the accuracy assessment. Kappa statistics and overall accuracy and were computed for all the images during the accuracy assessment.

2.5. Change detection

Change detection is the process of observing the differences that have taken place in the state of an object, viewed at different periods. To analyze the changes in the land cover, post-classification change detection was used. The reason for using post-classification change detection is that it provides comprehensive information on changes that occurs in a class cover to other classes concerning the place of change, the extent, and the amount of the change (Stemn et al., 2014; Acheampong et al., 2018). The post-classification change detection was conducted in QGIS and it was employed to determine changes in the land cover in three intervals (1991–2002, 2002–2008, and 2008–2018).

2.6. Urban sprawl measurement

Urban sprawl throughout 1991 to 2018 was measured by the use of Shannon entropy together with GIS tools. Before the measurement of sprawl was carried out, built-up images were extracted from the classified images to obtain urban built-up images. The raster calculator in QGIS was used to extract build-up images from 1991 to 2018 and then

Table 2
A classification scheme for land cover classes.

Land cover class	Explanation
Water	This includes the rivers, streams, and lakes in the study area.
Bare land	They are opened spaces whose soil surfaces are exposed. They have no vegetative cover or impervious surface.
Vegetation	This includes farmlands/ agricultural lands and forest areas. Land used primarily for production of food and fiber, Cropland, pasture, and other commercial and horticultural crops
Built-up or Settlement	This includes built-up areas or areas covered by made-made structures. Within this category are residential areas, industrial areas, and commercial areas.

reclassified the images into build-up and non-build-up. Thirteen concentric or multiple ring buffer zones were generated around a chosen center point. The central business district, Takoradi market circle was chosen as the center point for generating the buffer zones. Studies have used different geometries for creating buffer zones; some use circular or concentric circles as buffer zones whereas others use multiple square buffers (Chong, 2017; Aswal et al., 2018). This study chose concentric circular buffer zones because it captures the shape of the study area effectively. The buffers were created at a distance interval of 1 km around the center point using QGIS. These interval distances were chosen because it covers the majority of the area within the metropolis. As part of Shannon's entropy calculation, the total number of pixels in each buffer, the amount of built-up in each zone, and the total number of built-up areas were computed. This was done using the zonal statistics tool in QGIS. The results of the zonal statistics for each year were saved and exported to the Microsoft Excel table where further calculations using the Shannon entropy formula were applied. Shannon Entropy measures the degree of dispersion or compactness of a spatial variable (Chong, 2017; Gupta et al., 2018; Mosammam et al., 2017). It is calculated by the following equations:

$$E_n = -\sum_i^n P_i \log\left(\frac{1}{P_i}\right) \quad (1)$$

From the Eq. (1), ln is the natural log, $P_{i\ \text{is the}}$ value of the geospatial variable in each zone divided by the total land area in that zone. Thus, the ratio of the spatial element in the ith zone is expressed in Eq. (2). n is the total number of zones.

$$P_i = \frac{x_i}{\sum_i x_i} \quad (2)$$

The Shannon entropy (E_n) values vary from 0 to the value of Log (n). When the value is closer to 0, the distribution of the variables is highly concentrated in one zone and if the value is closer to log (n), the distribution is dispersed (Gupta et al., 2018). However, it more suitable to rescale the entropy value into the range of 0 and 1. This can be done by computing the relative entropy (E_n') which is expressed in Eq. (3).

$$E_n' = -\sum_i^n P_i log\left(\frac{1}{P_i}\right)/log(n) \quad (3)$$

.A flowchart that summarizes the methodology is presented in Fig. 2.

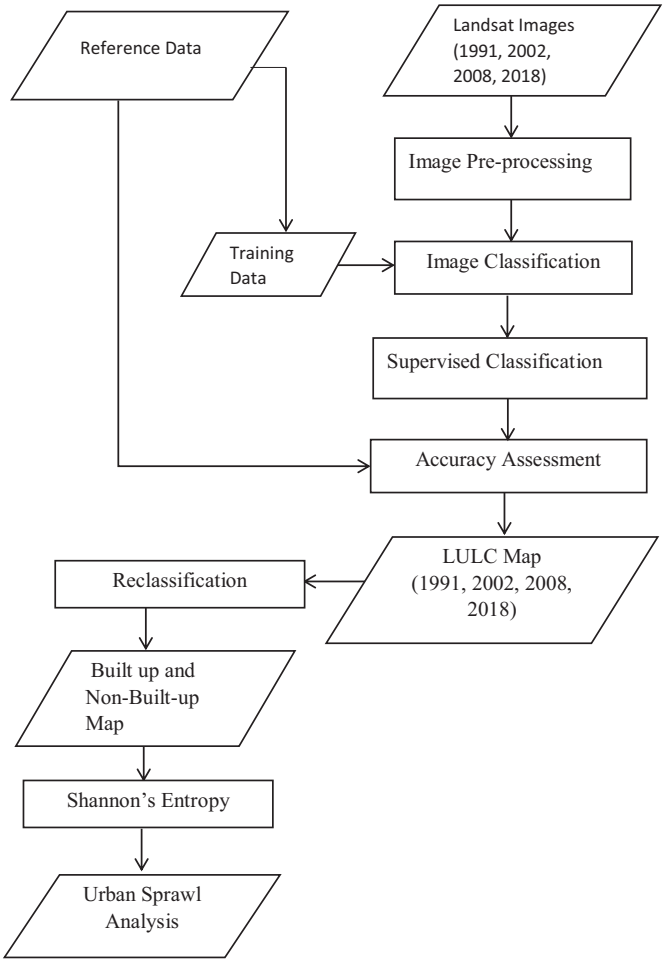

Fig. 2. Flowchart of research methodology.

3. Results and discussions

3.1. Land use land cover maps

As shown in Fig. 3, 1991, 2002, 2008, and 2018 images of the study area were classified into four classes, namely; water, vegetation, settlement, or built-up and bare lands. These classes, according to Table 4.1, in the year 1991; water covered an area of 5.35 km^2 representing (3.06%) of the total area, vegetation covered 137.20 km^2 representing (78.51%) of the total area, settlement covered an area of 8.55 km^2 representing (4.89%) of the total area and bare lands covered 23.65 km^2 representing (13.54%) of the total area. From Table 3 and Fig. 3, vegetation covered the highest land area and water covered the least land area. The classified results of the 2002 image presented in Table 3 showed a decrease in water to 5.32 km^2 representing about 3.04%, vegetation decreasing to 135.80 km^2 representing 77.71%, settlement increasing to 11.50 km^2. representing 6.58% and bare land reducing to 21.27 km^2 representing 12.72%. From the results, though vegetation has the highest land area, comparing it to the 1991 classified image, there was a decrease in its land area. The same can be said of bare land and water which decreased in 2002. The decrease in these land cover types led to a substantial increase in settlement. In 2008, water covered an area of 5.71 km^2 representing about 3.28%, vegetation covered an area of 130.77 km^2 representing 75.03%, settlement covered an area of 24.73 km^2 representing 14.19%, and bare land covered 13.07 km^2 representing about 7.50%. From the 2008 classified map, there was a decrease in the area of vegetation and bare lands whereas water and settlement increased considerably in the same year. Expansion in settlement or built-up and water took place by taking portions of land area occupied by the two classes. There was a considerable increase in settlement or built-up owing to the decrease in the three classes. Observing from Table 3, the 2018 classified map had water covering an area of 5.19 km^2

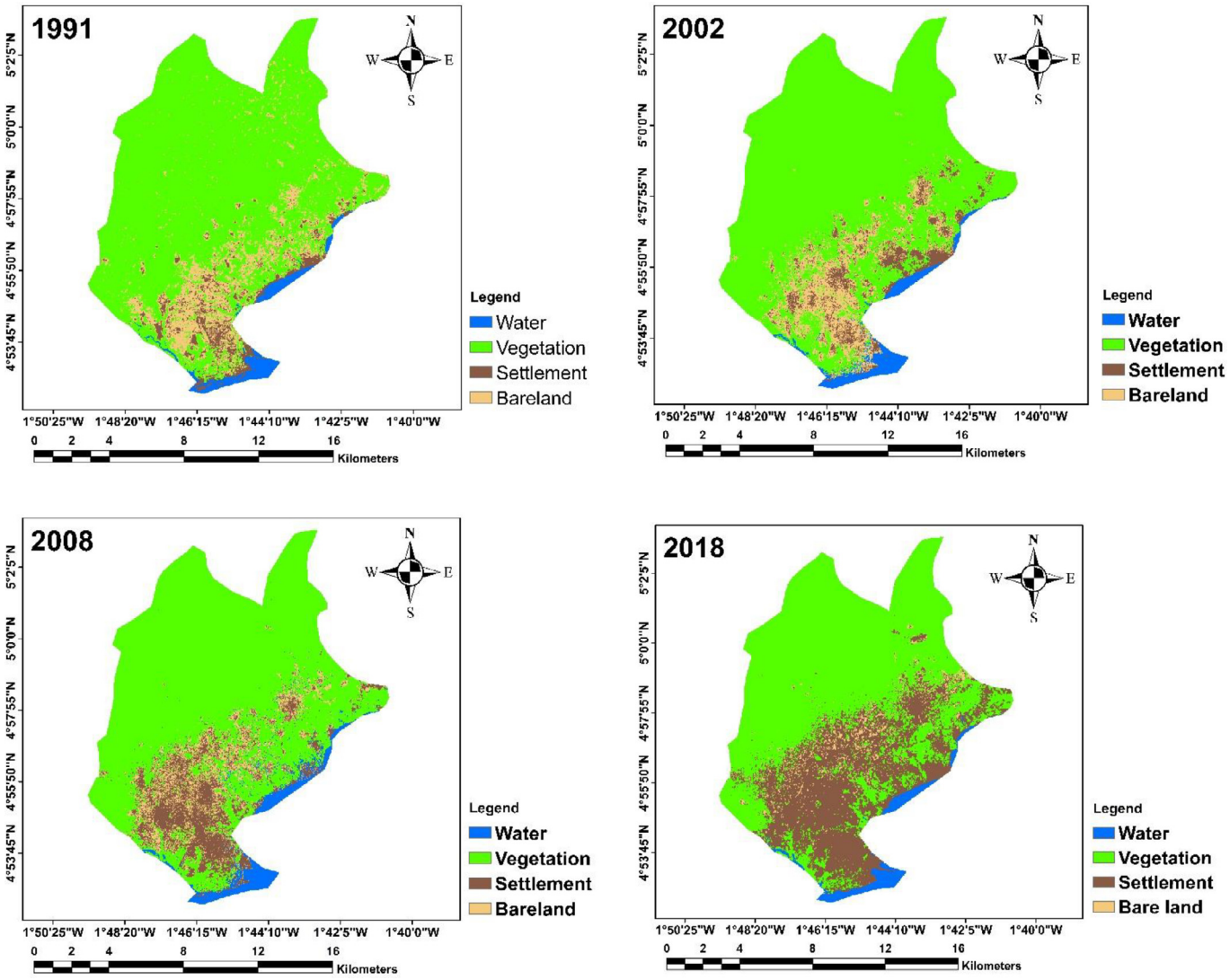

Fig. 3. Land use land cover changes from 1991 to 2018.

Table 3
Area coverage of the land cover classes.

Land cover class	1991		2002		2008		2018	
	Area (Km^2)	Area (%)	Area (Km^2)	Area (%)	Area (Km^2)	Area (%)	Area (Km^2)	Area (%)
Water	5.35	3.06	5.32	3.04	5.71	3.28	5.19	2.98
Vegetation	137.20	78.51	135.80	77.71	130.77	75.03	108.82	62.43
Settlement	8.55	4.89	11.50	6.58	24.73	14.19	53.85	30.90
Bare land	23.65	13.54	21.27	12.72	13.07	7.50	6.43	3.69
Total Area	***174.75***	***100***	***174.76***	***100***	***174.74***	***100***	***174.75***	***100***

representing 2.98%, vegetation covered an area of 108.82 km^2 representing 62.43%, settlement covered an area of 53.85 km^2 representing 30.90% and bare land covered an area of 6.43 km^2 representing 3.69%. As shown clearly in Fig. 3 and from Table 3, vegetation occupies the highest land area, whereas water, still has the lowest area coverage. Comparing the 2018 classified map to the 2008 classified map, it can be seen that, in 2018, there was a reduction in the area coverage of water, vegetation, and bare land. Settlement was the only class that had an increase in its area coverage. This indicates that building and construction have increased significantly over the years. Also, transitioning from 1991 to 2018, there has been a persistent increase in settlement while some of the classes have had an inconsistent or irregular increase or decrease in their land cover. Water, for instance, increased in 2002 but decreased in 2008 and 2018. Vegetation and bare lands, however, decreased throughout the years. Table 3 shows the area coverage of each class of the various years in square kilometers (km^2) and percentage.

3.2. Accuracy assessment

Accuracy assessment is essential in determining the quality of classification used for change detection and urban change analysis. The accuracy of the various classified maps was computed through the use of the error matrix and Kappa statistic. Error matrix is a table with classified data at the rows and reference data at the columns (Othow et al., 2017). Four hundred and eighty reference data were used to compute for the accuracy assessment of the classified maps. The overall accuracy

Table 4
Assessment of classification accuracy.

Year	User's accuracy (%)				Producer's accuracy (%)				Overall accuracy (%)	Kappa coefficient (%)
	Water	Vegetation	Settlement	Bare Land	Water	Vegetation	Settlement	Bare Land		
1991	100.00	93.75	80.64	81.48	100.00	100.00	83.00	73.00	89.16	85.55
2002	100.00	100.00	58.97	65.21	93.33	100.00	76.66	50.00	80.00	73.33
2008	96.55	85.71	71.79	94.11	93.33	100.00	93.33	53.33	85.00	80.00
2018	100.00	76.92	73.80	100.00	80.64	100.00	100.00	53.33	83.60	78.13

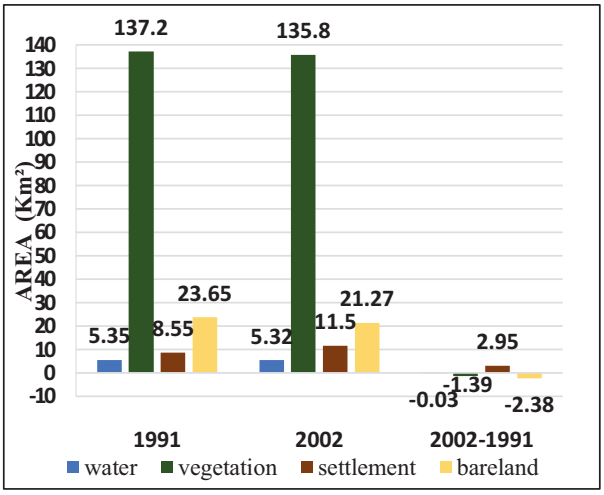

Fig. 4. : Trend of change from 1991 to 2002.

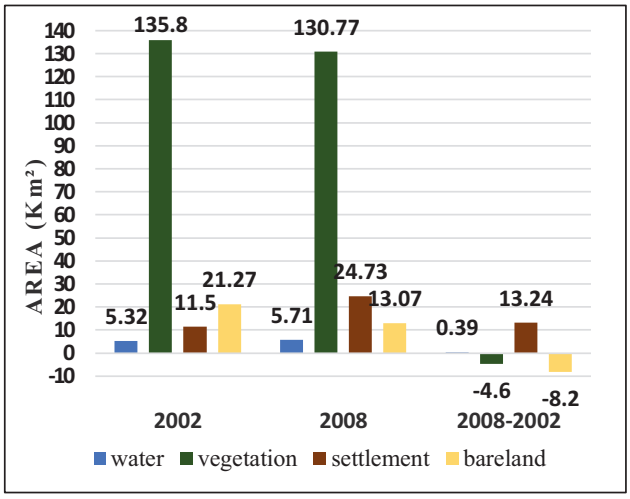

Fig. 5. : Trend of change from 2008 to 2018.

for 1991 was found to be 89.16%, 2002 was found to be 80.00%, 2008 was found to be 85.00%, and 2018 was found to be 83.60%. Kappa Coefficient for the classified maps of 1991, 2002, 2008, and 2018 was respectively determined to be 85.55%, 73.33%, 80.00%, and 78.13%. The results of the accuracy assessment are summarized in Table 4.

3.3. The trend of land use land cover changes from 1991 to 2018

Trend analysis on land use and land cover indicates where the land cover types are changing to. In this study, this was done by using the initial years of comparison as the base. Between 1991 and 2002, water decreased by 0.03 km^2, vegetation decreased by 1.39 km^2, settlement increased by 2.95 km^2 and bare land decreased by 2.38 km^2 (Fig. 4). From the results, even though, vegetation and water were reduced, bare land reduced substantially whereas settlement had a substantial increase. The

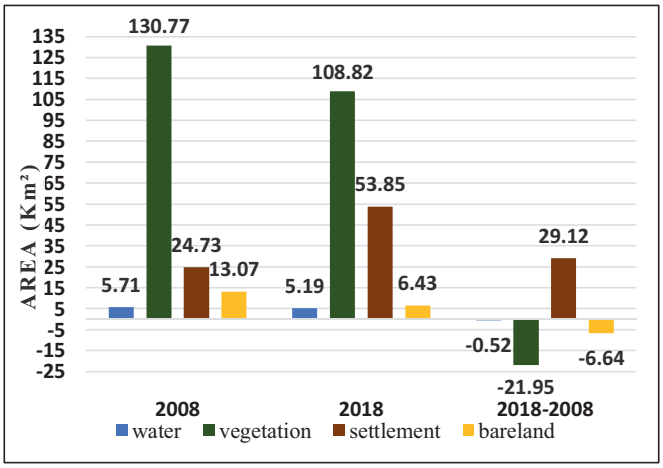

Fig. 6. : Trend of change from 2008 to 2018.

substantial increase in settlement indicates the conversion of most of the land cover types into impervious surfaces. Hence, showing that urban expansion is taking place within the metropolis.

From 2002 to 2008, the magnitude of water increased by 0.39 km^2, vegetation reduced by 4.60 km^2, settlement, however, increased by 13.24 km^2 and bare land decreased by 8.20 km^2 (Fig. 5). According to the results, settlement and water had an increase whereas the rest of the classes saw a decrease in the area coverage. The increase in water was due to the flooding which took place in the years, 2006, 2007, and 2008 (Stemn et al., 2014). During those years, areas susceptible to flooding such as the Wetland located around New Takoradi, Wetland near Aboadze thermal plant, and areas close to the Whin River were covered with water. Also, during the flooding period, the Whin River overflowed its banks and claimed several hectares of other land cover types. Moreover, in the year 2008, expansion works by the Ghana Water Works to increase the supply of drinkable water within the metropolis were going on in Inchaban, and this claimed a lot of vegetative land and farmlands into water. On the other hand, the increase in settlement, coupled with other factors can be attributed to the discovery of oil in commercial quantities in 2007. The discovery and production of oil attracted not only companies and industries into the metropolis, but also increased the population of migrants who came to look for employment (Adarkwa, 2012; Fiave, 2017; Eduful and Hooper, 2019). For instance, in 2000, when the oil had not been discovered, the population of the metropolis was 359, 363. After the discovery of oil, the population increased tremendously to 559, 548 in 2010 (Service, 2014). These companies and the increased population require land for industry and residential purposes, hence increasing build-up. The trend of change in the classes from 2002 to 2008 indicates the prevalence of urban expansion through increased construction of buildings and impervious surfaces. As a result of this, portions of the other classes were converted to settlement or build-up.

Generally, when the use of land in an urban center is changing from vegetation cover to other land uses, build-up or settlement becomes the dominant land use. The changing trend in the classes between 2008 and 2018 is evidence of build-up being predominant in the change of vegetative class to other land classes. Observing from Figure 6, it can be seen

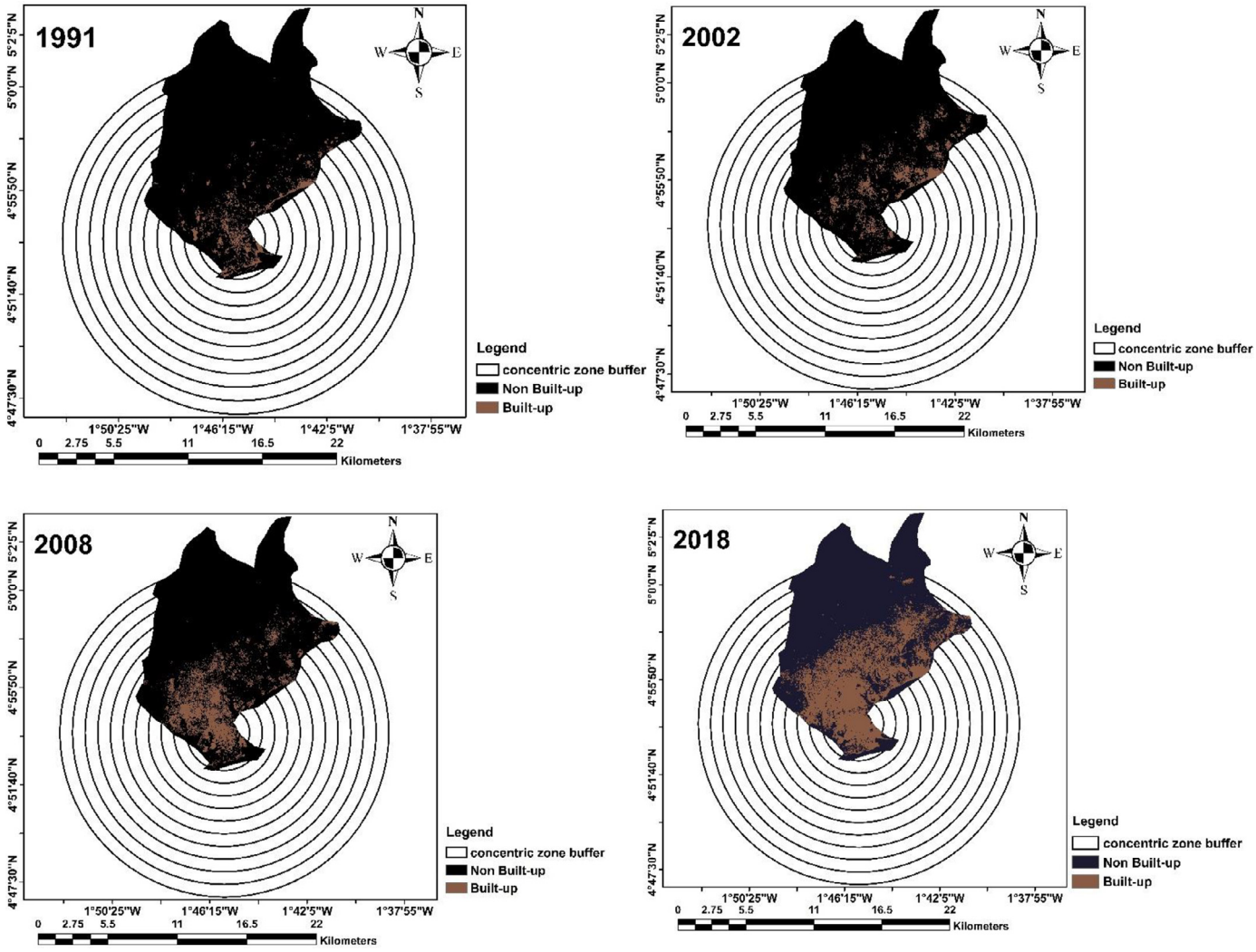

Fig. 7. Reclassified maps showing Built-up and Non-Built-up areas for the years;199, 2002, 2008, and 2018.

that settlement or build-up has increased tremendously by 29.12km^2. The high increase in settlement or build-up is due to the conversion of other land cover types into impervious surfaces. Owing to the increased population through the oil discovery, there was pressure on the demand for land for accommodation, setting up of businesses and offices within the city. This, therefore, prompted a response from real estate developers of which there has been the development of new housing like the Takoradi Oil Village and the King City. Moreover, existing establishments such as Raybow Hotel, Hillcrest Hotel, Planter Lodge were expanded in 2012 to increase their intake while new establishments are springing up. The Raybow Hotel, for example, has expanded its establishment to accommodate over sixty (60) apartments whereas Planters Lodge has also redeveloped to 45 rooms. Also, the location of Protea Hotel, established in 2015 with 135 rooms, for instance, used to be bare land with parts covered with vegetation. Best Western Plus Atlantic Hotel, established in 2012, was also previously covered with vegetation, but due to the increased demand for accommodation and urban space, it has now been turned into a built-up. In 2010, there was a plan by the department of urban road to develop alternative routes and to expand some existing single road lanes into double lane roads in the city. This saw the construction of the Kansaworado bypass (now called N1), but its construction converted the land cover types into impervious surfaces (Fiave, 2017). The expansion of the Takoradi port which started in November 2014, according to the Ghana Ports and Harbour (GPHA) affected about 53,000 hectares of arable land of New Takoradi and Poase (Stemn et al., 2014). These have given rise to build-up. The magnitude of water, vegetation, and bare land respectively decreased by 0.52km^2, 21.95km^2, and 6.64km^2 (Fig. 6). The decrease in water in comparison to the immoderate increase in built-up further reveals that people have encroached the water areas for construction purposes. In the study of Aduah et al. (2013), it was revealed that waterways within the metropolis were been converted into built-up. A situation like this hinders a city from enjoying the benefits linked with conserving water and also makes it prone to flooding because the water would not have a way of entering into the sea especially during a heavy downpour. Also, contributing to the reduction in water is the activities of quarry agencies within the metropolis. The Anankori river, for instance, has some of its tributaries being filled and blocked with boulders to enable heavy-duty trucks to carry the quarry or boulders from the river. Report by, the daily Graphic indicates that Anankori River is the main source of water for the metropolis, but the activities of the quarry agencies have affected the quality and amount of water from the Anankori River. Therefore, the supply of water within the metropolis has reduced.

3.4. Urban sprawl analysis

To analyze the nature and pattern of urban sprawl, the land cover maps of 1991, 2002, 2008, and 2018 were first reclassified into build-up and non- build-up as shown in Fig. 7. It is observed from Fig. 7 that built-up increased from 1991 to 2018, and is highly con-

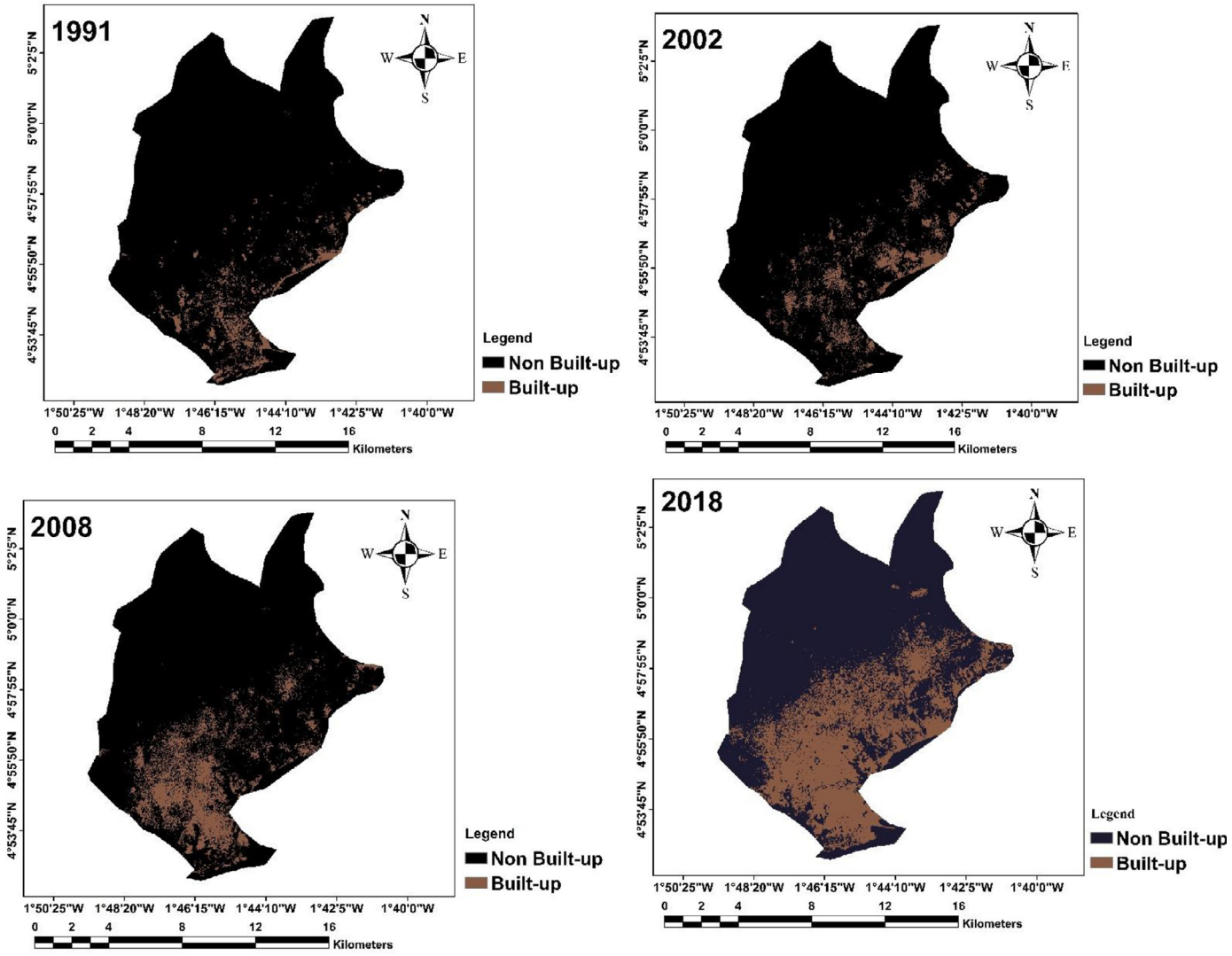

Fig. 8. Concentric ring buffer of reclassified maps for the years: 1991, 2002, 2008, and 2018.

Table 5
Expansion of built-up area of Sekondi-Takoradi.

Year	Total area (km^2)	Area of built-up (km^2)	Area of built-up (%)	Change in built-up areas (km^2)
1991	174.75	8.55	4.89	–
2002	174.76	11.50	6.58	2.95
2008	174.74	24.75	14.16	7.58
2018	174.75	53.87	30.83	16.67

centrated at the south-western and eastern part of the study area (due to the presence of the Market Circle, which is the Central Business Center).

From Table 5, it could be seen that there have been significant changes in the built-up from 1991 to 2018. The built-up area increased from 8.55km^2 to 53.85km^2 between the period 1991 and 2018. In 1991, the total land area was 174.75 km^2: the built-up area was 8.55 km^2 and the non-built-up covered an area of 166.2 km^2. The population in 1991 was 244,000. In 2002, the total land area of the study was 174.76 km^2, built-up covered an area of 11.50 km^2, non-built-up marked the area of 163.26 km^2 and the population was 331,000. The total land area for 2008 was 174.74 km^2, built-up and non-built-up respectively covered an area of 24.73 km^2 and 150.01 km^2 and there was a population of 473,000. The study's land area in 2018 was 174.75 km^2 and had a population of 855,000. 53.85 km^2 of the total area in 2018 was built-up land and 120.9 km^2 was non-built-up land. The changes in built-up from the year 1991 to 2018 are summarized in Table 5.

Second, with a concentric circle of 1 km intervals starting from the city center, the reclassified built-up and non-built-up images were divided into thirteen buffer zones. This was to help in identifying the direction of urban land development (Mundhe et al., 2015) and to quantify sprawl for the various years. Fig. 8 shows the thirteen zones with a concentric circle of 1 km intervals that were used to compute the level of sprawl within various years.

The build-up density values in each zone, the Shannon entropy values, and the relative Shannon entropy values were calculated for the various years of the study. The results are presented in Table 5.

Table 6 shows an undulating increase and decrease in the values of entropy, although, the entropy value for each year was relatively high. The differences in the entropy values are insignificant since the values

Table 6
Values of relative and Shannon's entropy.

Year	Built-up area (km^2)	Shannon's entropy value	Relative Shannon's entropy value
1991	8.55	2.50	0.97
2002	11.50	2.42	0.95
2008	24.75	2.46	0.96
2018	53.87	2.42	0.94
Log (13)		2.56	1

differ throughout the years by less than 1%. This shows that for the twenty-seven (27) years, there has not been a considerable change in the entropy values. Log (13), which is 2.56 is the highest Shannon entropy value, and 2.50, 2.42, 2.46, and 2.42 are respectively Shannon's entropy values for the four periods. From the relative Shannon entropy, (which is scaled from the value of 0 to 1 with 0 as minimum and 1 as maximum), it is observed that the values 0.97, 0.95, 0.96, and 0.94 were high for all the years. The minimum value of 0.94 was in the year 2018 and the maximum value of 0.97 was in the year 1991. These values are closer to 1, and according to Mosammam et al. (2017), indicates that the city is sprawled. Therefore, from 1991 to 2018 urban sprawl has been high in the city. Ssprawl was high in 1991 but decrease in 2002 and increased in 2008 and then decrease again in 2018. This indicates that in the year 1991 the city was more sprawled as compared to the other years. With the fact of the city experiencing high dispersion, the spatial distribution of infrastructures and provision of basic amenities such as roads, water, electricity, and schools, etc. will be difficult. It is, therefore, necessary as suggested by Aduah et al. (2013), for the city's planning authorities to adopt and employ suitable sustainable planning methods that fit every aspect of the city to ensure efficient utilization of the limited land resource and to control the rate of urban dispersion.

4. Conclusion

GIS and remote sensing techniques were used to examine and determine changes that took place in the study area from 1991 to 2018. Results of the study showed considerable change in the land covers in which settlement or built-up had an average yearly increment over the 27years (from 1991 to 2018). Water, however, decreased from 1991 to 2002, but increased in 2008 and decreased in 2018. Vegetation and bare land showed a constant decrease from 1991 to 2018. Increasing urban population and its associated demand for residential, industrial and commercial purposes was identified as the major factor behind the increase in settlement and built-up. This, undoubtedly, support the notion that human activities or anthropogenic activities greatly affect the earth's surface. The study also used Shannon's entropy to measure urban sprawl. Values of entropy for the years of 1991, 2002, 2008, and 2018 revealed that Sekondi-Takoradi is sprawling, and at the time of 1991, the city was more sprawled compared to years 2002, 2008, and 2018. Urban sprawl measurements aids in formulating policies and regulations that would help deal with the dominant form. A major limitation of the study was the availability of cloud-free Landsat images for the required time-points of the study area. This, however, led to inconsistency in the time interval of the images used. Also, Landsat images are to a limited extent coarse and unable to identify changes on small scale. So, for effective and more accurate classification of LULC classes to be achieved, future studies may consider using high-resolution imageries such as Sentinel, IKONOS, and QUICKBIRD. Moreover, future works should consider other variables such as climate, policies, and regulations that affect LULC changes.

Declaration of Competing Interest

The authors declare no conflict of interest.

Author contributions

Ernest Biney developed the concept of the manuscript and Ebenezer Boakye contributed by content and expertise. The findings, discussions, and manuscript writing were all contributed by all authors.

No funding

This research did not receive any specific grant from funding agencies, commercial or from profit sectors.

References

Acheampong, M., Yu, Q., Enomah, L.D., Anchang, J., Eduful, M., 2018. Land use/cover change in Ghana's oil city: assessing the impact of neoliberal economic policies and implications for sustainable development goal number one–a remote sensing and GIS approach. Land use policy 73, 373–384. doi:10.1016/j.landusepol.2018.02.019.

Adarkwa, K.K., 2012. The changing face of Ghanaian towns. Afr. Rev. Econ. Finance 4 (1), 1–29.

Adjei Mensah, C., Kweku Eshun, J., Asamoah, Y., Ofori, E., 2019. Changing land use/cover of Ghana's oil city (Sekondi-Takoradi Metropolis): implications for sustainable urban development. Int. J. Urban Sustain. Dev. 11 (2), 223–233. doi:10.1080/19463138.2019.1615492.

Aduah, M.S., Baffoe, P.E., 2013. Remote sensing for mapping land-use/cover changes and urban sprawl in Sekondi-Takoradi, Western Region of Ghana. Int. J. Eng. Sci. 2 (10), 66–72.

Aduah, M.S., Mantey, S., 2020. Modelling potential future urban land use changes in the Sekondi-Takoradi metropolitan area of Ghana. Ghana J. Technol. 4 (2), 26–32.

Appiah, D.O., Forkuo, E.K., Bugri, J.T., Apreku, T.O., 2017. Geospatial analysis of land use and land cover transitions from 1986–2014 in a peri-urban Ghana. Geosciences 7 (4), 125. doi:10.3390/geosciences7040125.

Assembly, S.T., 2010. Draft Medium-Term Development Plan (2010–2013).

Aswal, P., Saini, R., Ansari, M.T., 2018. Spatio Temporal Monitoring of Urban Sprawl using GIS and Remote Sensing Technique. Int. J. Comput. Appl. 182 (27), 11–24.

Chatwin, M., Arku, G., 2018. Co-creating an open government action plan: the case of Sekondi-Takoradi metropolitan assembly, Ghana. Growth Change 49 (2), 374–393. doi:10.1111/grow.12234.

Chong, C.H.S., 2017. *Comparison of Spatial Data Types for Urban Sprawl Analysis Using Shannon's Entropy* (Doctoral Dissertation. University of Southern California.

Dominguez, J., de Guzman, F., Reandelar Jr., M., Thi Phung, T.K., 2018. Prevalence of dementia and associated risk factors: a population-based study in the Philippines. J. Alzheimer's Dis. 63 (3), 1065–1073. doi:10.3233/JAD-180095.

Eduful, A.K., Hooper, M., 2019. Urban migration and housing during resource booms: the case of Sekondi-Takoradi, Ghana. Habitat Int 93, 102029.

Fiave, R.E., 2017. Sekondi-Takoradi as an oil city. Geogr. Res. Forum 37 (December), 61–79.

Garg, V., Nikam, B.R., Thakur, P.K., Aggarwal, S.P., Gupta, P.K., Srivastav, S.K., 2019. Human-induced land use land cover change and its impact on hydrology. HydroResearch 1, 48–56. doi:10.1016/j.hydres.2019.06.001.

Gupta, S., Islam, S., Hasan, M.M., 2018. Analysis of impervious land-cover expansion using remote sensing and GIS: a case study of Sylhet sadar upazila. Appl. Geogr. 98, 156–165. doi:10.1016/j.apgeog.2018.07.012.

Guzmán, P.C., Roders, A.P., Colenbrander, B.J.F., 2017. Measuring links between cultural heritage management and sustainable urban development: an overview of global monitoring tools. Cities 60, 192–201. doi:10.1016/j.cities.2016.09.005.

Hong, H., Miao, Y., Liu, J., Zhu, A.X., 2019. Exploring the effects of the design and quantity of absence data on the performance of random forest-based landslide susceptibility mapping. Catena 176, 45–64.

Li, J., Wang, Z., Lai, C., Wu, X., Zeng, Z., Chen, X., Lian, Y., 2018. Response of net primary production to land use and land cover change in mainland China since the late 1980s. Sci. Total Environ. 639, 237–247.

Mohamed, M.A., Anders, J., Schneider, C., 2020. Monitoring of Changes in Land Use/Land Cover in Syria from 2010 to 2018 Using Multitemporal Landsat Imagery and GIS. Land 9 (7), 226. doi:10.3390/land9070226.

Mosammam, H.M., Nia, J.T., Khani, H., Teymouri, A., Kazemi, M., 2017. Monitoring land use change and measuring urban sprawl based on its spatial forms: the case of Qom city. Egypt. J. Remote Sens. Space Sci. 20 (1), 103–116. doi:10.1016/j.ejrs.2016.08.002.

Mundhe, N.N., Jaybhaye, R.G., 2015. Measuring urban growth of pune city using shannon entropy approach. J. Geogr. Geol. 119 (290), 302.
Obeng-Odoom, F., 2014. Urban land policies in Ghana: a case of the emperor's new clothes? Rev. Black Polit. Econ. 41 (2), 119–143 10.1007%2Fs12114-013-9175-5.
Obeng-Odoom, F., 2019. Oil, local content laws and paternalism: is economic paternalism better old, new or democratic? Forum Soc. Econ. 48 (3), 281–306.
Othow, O.O., Gebre, S.L., Gemeda, D.O., 2017. Analyzing the rate of land use and land cover change and determining the causes of forest cover change in Gog district, Gambella regional state, Ethiopia. J. Remote Sens. GIS 6 (4), 218. doi:10.4172/2469-4134.1000219.
Service, G.S., 2014. Ghana Living Standards Survey Round 6 (GLSS 6).: Poverty Profile in Ghana (2005-2013). Ghana Statistical Service.
Stemn, E., Agyapong, E., 2014. Assessment of urban expansion in the Sekondi-Takoradi Metropolis of Ghana using remote-sensing and GIS approach. Int. J. Sci. Technol. 3 (8), 452–460.
Tarkang, E.E., Lutala, P.M., Dzah, S.M., 2019. Knowledge, attitudes and practices regarding HIV/AIDS among senior high school students in Sekondi-Takoradi metropolis, Ghana. Afr. J. Prim. Health Care Fam. Med. 11 (1), 1–11. doi:10.1186/s12889-016-3516-9.
Wandl, A., Magoni, M., 2017. Sustainable Planning of Peri-Urban Areas: Introduction to the Special Issue doi:10.1080/02697459.2017.1264191.
Yang, Y., Liu, Y., Li, Y., Du, G., 2018. Quantifying spatio-temporal patterns of urban expansion in Beijing during 1985–2013 with rural-urban development transformation. Land use policy 74, 220–230. doi:10.1016/j.landusepol.2017.07.004.
Yu, D., Xie, P., Dong, X., Su, B., Hu, X., Wang, K., Xu, S., 2018. The development of land use planning scenarios based on land suitability and its influences on eco-hydrological responses in the upstream of the Huaihe River basin. Ecol. Modell. 373, 53–67. doi:10.1016/j.ecolmodel.2018.01.010.
Zhou, X., Chen, H., 2018. Impact of urbanization-related land use land cover changes and urban morphology changes on the urban heat island phenomenon. Sci. Total Environ. 635, 1467–1476. doi:10.1016/j.scitotenv.2018.04.091.